

Surfactant-assisted Pulse Electrodeposition of Hausmannite Nano-rods/particles with Improved Pseudocapacitive Performance

Mustafa Aghazadeh

Materials and Nuclear Research School, Nuclear Science and Technology Research Institute (NSTRI), P.O. Box 14395-834, Tehran, Iran

Received: January 07, 2018, Accepted: February 28, 2018, Available online: July 31, 2018

Abstract: Pulse cathodic electrodeposition of manganese oxide was performed from 0.005M $MnCl_2$ in the presence of cetyl trimethylammonium bromide (CTAB). The electrosynthesis experiments were done at the simple pulse mode ($t_{on}=1ms$ and $t_{off}=1ms$) with applying current density of $10 mA cm^{-2}$. The structural analyses through XRD and FTIR revealed that the prepared sample have the pure hausmannite crystal structure. Morphological observations by SEM showed that the deposited hausmannite has mixed rod/particle morphology. The charge storage performances of the prepared hausmannite were evaluated by cyclic voltammetry and charge-discharge techniques. The Mn_3O_4 working electrode exhibited only 13% capacity decay after 1000 cycles at the current load of $2 A g^{-1}$, and its SC value reduced from $239 F g^{-1}$ to $207 F g^{-1}$. The results proved that the prepared Mn_3O_4 nano-rods/particles are suitable electrode material for supercapacitors.

Keywords: Pulse electrodeposition; Hausmannite; Nano-rods/particles; Pseudocapacitive performance

1. INTRODUCTION

Rapid expansion in the global energy consumption of fossil fuels and the world's population explosion, have led to an urgent necessity for the development of alternative green energy sources. Electrochemical energy storage and conversion systems are the most important case as a provider of sustainable energy technologies in foreseeable future [1]. Among electrochemical energy storage devices, supercapacitors are highly potential energy storage candidates especially where high power density is favorable. Unlike conventional energy storage systems such as batteries, supercapacitors not only charge rapidly but also are more durable due to their indefinite cycle life, non-vulnerability to temperature change, and non-toxicity in nature. Various materials including carbonaceous materials, conducting polymers, and transition-metal oxides have been applied as an electrode material in supercapacitors [2]. Among them metal oxides and hydroxide like NiO [3-9], Ni(OH)₂ [10-13], Co₃O₄ [14-20], SnO₂ [21], Co(OH)₂ [22-28], MnO₂ [29-33], Mn₃O₄ [34-37], and Fe₃O₄ [38,39], possess high specific capacitance and excellent reversibility because of the ideal solid-state pseudo-faradic reactions. Among these electro-active materials, Mn-based electrodes have attracted much attention as a pseu-

docapacitive material, owing to its appealing features, including natural abundance, low cost, and environmental friendliness as well as high theoretical specific capacitances (SC) [40-42]. However, the reported SC values in the literature are in the limited area of 150–250 F/g which is referred to the low Na⁺ or H⁺ diffusion to manganese oxide structure and its poor electrical conductivity [41]. In this regard, many researchers have focused on the preparation of nanostructures with specific morphology to dispel these restrictions.

In this work, we report hausmannite nano-rods/particles prepared through a novel and one-pot procedure i.e. pulse surfactant-assisted cathodic electro-deposition. The charge storage capability of prepared nanostructures as supercapacitor electrode materials is also investigated. The preparation method includes one-pot from galvanostat deposition from 0.005M manganese chloride aqueous bath in the presence of an cationic surfactant (i.e. cetyl trimethylammonium bromide, CTAB). Notably, pulsed CTAB-assisted cathodic electrosynthesis of manganese oxide has not been investigated until now. The pure Mn₃O₄ crystal phase and its nano-rod/particle morphology of the prepared products are confirmed through XRD, Ft-IR, DSC and FE-SEM analyses. The cyclic voltammetric and galvanostatic charge-discharge data are also proved the high supercapacitive performance of the prepared nano-rods/particles as supercapacitor electrode material.

*To whom correspondence should be addressed: Email: maghazadeh@aeoi.org.ir
Phone:

2. EXPERIMENTAL SECTION

2.1. Chemicals

MnCl₂ · 6H₂O, polyvinylidene fluoride (PVDF, Mw ~180,000), N-Methyl-2-pyrrolidone (NMP), cetyl trimethylammonium bromide (CTAB), carbon black and Na₂SO₄ were purchased from Sigma-Aldrich and used as received. All solutions were prepared using water purified by a UHQ Elga System. An aqueous solution of 5 mM MnCl₂ · 6H₂O was prepared for electrodeposition.

2.2. Preparation of oxide samples

Mn₃O₄ nanorods were prepared via a one-step process, including the initial step of cathodically electrodepositing manganese oxide from chloride bath at a pulse current (PC) mode in a typical on-times and off-times ($t_{on}=1ms$ and $t_{off}=1ms$) with a peak current density of 10 mA cm⁻² ($I_a=10$ mA cm⁻²). The bath solution was aqueous solution of 5 mM MnCl₂ · 6H₂O and 0.5cmc CTAB as an additive. The deposition time and bath temperature were 60 min and 25 °C, respectively. Prior to each deposition, the steel substrates were given a galvanostatically electropolishing treatment. The deposition experiments were conducted using an electrochemical workstation system (Potentiostat/Galvanostat, Model: NCF-PGS 2012, Iran). After the deposition, the steel substrates were repeatedly rinsed with water, and then dried at 50 °C for 5h. Finally the deposits were scraped from the substrates and evaluated by further analyses.

2.3. Characterization

The morphology of the prepared black powder was observed by field-emission scanning electron microscopy (FE-SEM, Mira 3-XMU with accelerating voltage of 100 kV). The crystal structure of the prepared powder was determined by X-ray diffraction of powder (XRD, Phillips PW-1800) using Cu K α radiation. FTIR spectra of the samples were obtained using a Bruker Vector 22 Fourier transformed infrared spectroscopy in the range of 400–4000 cm⁻¹. The thermal behavior analyses were also conducted under an N₂ atmosphere between the room temperature and 600 °C at a heating rate of 5°C min⁻¹ using an STA-1500 Thermoanalyzer system.

2.4. Electrochemical measurements

Cyclic voltammetry (CV) and galvanostatic charge–discharge (GCD) tests were done on a potentiostat (AUTOLAB®, Eco Chemie, PGSTAT 30). A three-electrode set-up used in the CV and GCD tests was constructed using the working electrode (Mn₃O₄ paste electrode), Ag/AgCl reference electrode (saturated with 1 M KCl), the counter electrode (platinum wire). All the electrochemical data were recorded in 1M Na₂SO₄ aqueous electrolyte. The Mn₃O₄ working electrode (WE) was made using the well-known paste procedure. In this way, the prepared Mn₃O₄ powder was physically mixed with acetylene black (>99.9%) and conducting graphite (with ratios of 75:10:10), and homogeneous black mixture was obtained. To this mixture, 5 wt.% of polyvinylidene fluoride (PVDF,) dissolved in N-Methyl-2-pyrrolidone (NMP) was added. After partially evaporating NMP, the resulting paste was pressed at 10 MPa to Ni foam (with 1 cm² area). The fabricated WE was dried for 5 min at about 150 °C in oven. The load of electroactive material on fabricated electrode was about 2.5 mg. The CVs of the fabricated WE were recorded in 1M Na₂SO₄ solution at the potential widow of 0 and 0.9 V vs. Ag/AgCl. The CV profiles

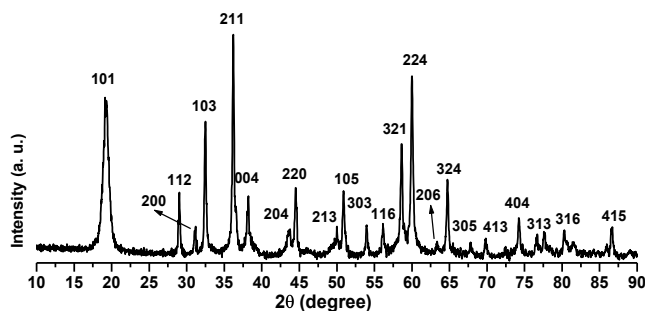


Figure 1. XRD pattern of the electro-synthesized product

were recorded at the various scan rates of 2, 5, 10, 20, 50 and 100 mV s⁻¹. The SCs of the WE were calculated from the CV profiles using Eq. (1) [14,15]:

$$C = \frac{Q}{m \Delta V}, \quad Q = \int_{V_2}^{V_1} I(V) dV \quad (1)$$

where C is the capacitance of cobalt hydroxide (F g⁻¹), Q is total charge, ΔV is the applied potential window, m is the mass of Mn₃O₄ powder (g) and $I(V)$ is a current response during the potential scan. The charge-discharge curves were provided at the different current loads of 0.5, 1, 2, 3 and 5 A g⁻¹ within a potential range of 0 to 0.9V vs. Ag/AgCl. The following formula was used to calculate the SCs of the fabricated WE [40]:

$$C = \frac{Q}{m \times \Delta V}, \quad Q = I \times \Delta t \quad (2)$$

where C is the calculated capacitance for fabricated WE, I is the applied current load (A), ΔV is the potential window (1 V), Δt is the time of a discharge cycle (s) and m is the mass of Mn₃O₄ (g).

3. RESULTS AND DISCUSSION

3.1. Structural characterizations

The XRD pattern of the electro-synthesized material is given in Fig. 1. All XRD peaks are perfectly matched to the tetragonal Mn₃O₄ pure phase. The lattice constants of the electrodeposited Mn₃O₄ are $a=5.753\text{\AA}$ and $c=9.436\text{\AA}$, which are consistent with those of bulk Mn₃O₄ (PDF File No. 24-734). No peak, relating to impurity phases like MnO₂ and Mn₂O₃, has been observed.

Morphological observations through SEM are shown in Fig. 2. In these images, two types of nanostructures i.e. rod and particle are seen for the electrodeposited manganese oxide. The Mn₃O₄ rods have uniform rod morphology with a narrow distribution of diameters. The observed rods are 50 nm in diameter and their length is in the range of 200-300nm. Also, the observed particles have relative uniform size distribution. The sizes of the deposited particles are very fine and are at a range of 20 nm. These uniformities implicate that the deposition and growth processes of the rods/particles on the cathode surface have proceeded with complete regularity and arrangement throughout all deposition time.

In order to have more information about the chemical bonds present in the electrodeposited manganese oxide, FT-IR spectrum

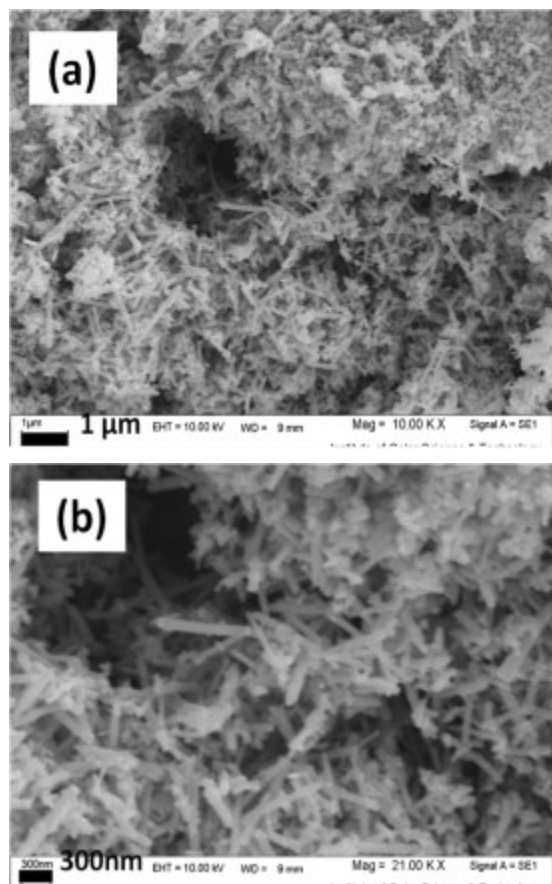


Figure 2. SEM images of the electrodeposited hausmannite

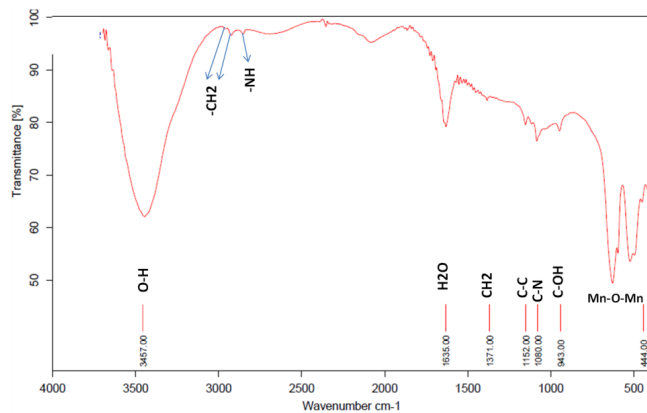


Figure 3. IR spectrum of the electro-synthesized hausmannite

of the electro-synthesized hausmannite was recorded in the wavelength range of 400-4000 cm^{-1} . Fig. 3 exhibits the FT-IR spectrum of the prepared products. In the range of 400-4000 cm^{-1} , several IR bands are seen at 2987, 2972, 2835, 1635, 1371, 1152, 1080, 943, 621, 517 and 444 cm^{-1} . The broad band at 3457 cm^{-1} is related to the -OH stretching vibration, and the band at 1635 cm^{-1} is corresponded to the bending vibrations of water molecules [20,34]. The

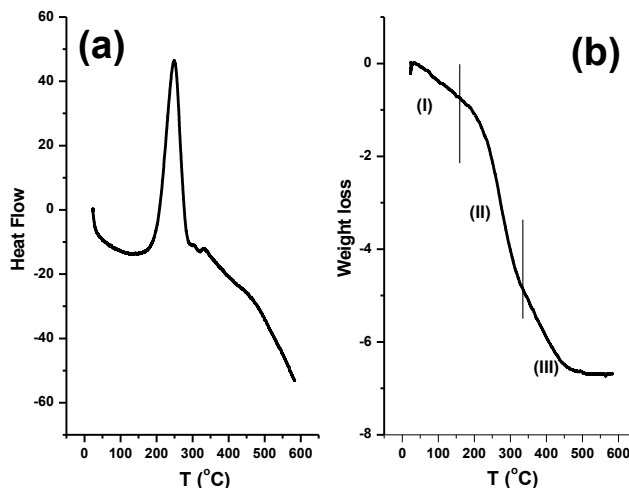


Figure 4. Thermogravimetric (DTA and TG) profiles of the electro-synthesized hausmannite

adsorption bands below 700 cm^{-1} i.e. 621, 517 and 444 cm^{-1} are due to the coupling between the Mn-O stretching modes of tetrahedral and octahedral sites, and indicative of the existence of octahedral MnO_6 [34,37]. A small band observed around 1371 cm^{-1} can be related to the bending vibration of O-H bonds connected with Mn atoms [37,42]. There are some new IR bands in Fig. 3, which are related to the vibrations modes of chemical bonds of CTAB i.e. C-C, CH_2 , C-N, C-O-H and -NH. These vibrations are (i) N-H stretching modes at 2835 cm^{-1} [43], (ii) C-N at 1080 cm^{-1} , (iii) C-C stretching vibration at 1152 cm^{-1} , [44], (iv) - CH_2 symmetric and asymmetric vibration at 2987 cm^{-1} and 2972 cm^{-1} , respectively [45]. These IR bands indicated the presence of CTAB adsorbed on the electro-synthesized hausmannite.

The thermal gravimetric (TG) and differential thermal analyses (DTA) analyses of the electro-synthesized Mn_3O_4 nano-material were performed between 25 and 600°C. Fig. 4 shows the DTA and related TG curves of our product. The TG profile has three step weight losses at the temperature ranges of (i) 25-150°C, (ii) 150-350°C and (iii) 350-500°C. In the temperature range of 25-150°C, the weight loss of 07.5%wt is due to the removal of weakly adsorbed H_2O molecules. The second weight loss of 4.25%wt can be related to the removal of the CTAB intercalated in the deposited oxide. The last weight loss (1.75%wt) can be assigned to the conversion of Mn_3O_4 to Mn_2O_3 [46]. After this step, the mass of sample is remained constant, and hence total weight loss of 6.75%wt is seen on the TG curve (Fig. 4b).

3.2. Capacitive performance of the electro-synthesized Mn_3O_4

The CV profiles of the fabricated Mn_3O_4 electrode were recorded between 0 and 0.9 V vs. Ag/AgCl at the various scan rates of 2, 5, 10, 20, 50 and 100 mV s^{-1} , and the resulted curves are shown in Fig. 5a. No peaks are present, indicating that the electrode is charged and discharged at a pseudo-constant rate over the complete voltammetric cycle. All voltammograms are close to rectangular in shape, which is indicative of the behavior of an double layer capacitor.

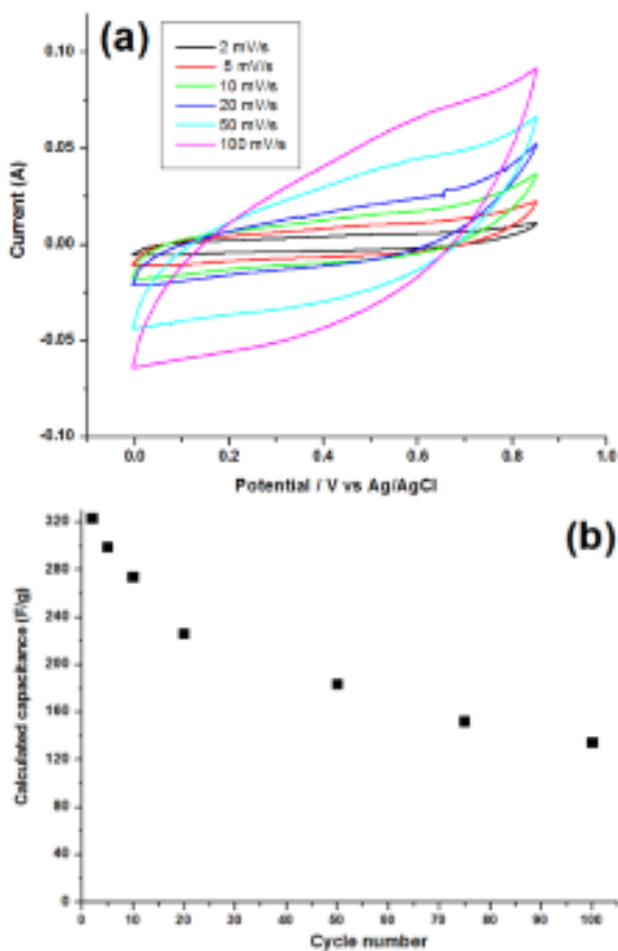


Figure 5. (a) Cyclic voltammograms of the fabricated hausmannite working electrode at the various scan rates and (b) corresponding calculated capacitances

As can be seen from Fig. 5a, the current under different current densities was slowly increased with scan rate, and the currents on all CV curves reaching plateau values very fast upon changing the direction of potential scan. These results revealed relative good electrochemical reversibility and a pseudo-capacitive behavior, which may be attributed to the high surface area and rod/particle arrangement of Mn_3O_4 deposit at the nanoscale. The SC values of Mn_3O_4 nano-rods/particles were through Eq. (1), and plotted versus the applied scan rates in the CV tests, as shown in Fig. 5b. It can be seen that this electrode is capable to deliver specific capacitances of 322, 298, 273, 217, 182, 152 and 134 F g^{-1} at the scan rates of 2, 5, 10, 25, 50 and 100 mV s^{-1} , respectively. These values verified good supercapacitive ability of the prepared Mn_3O_4 nano-rods/particles. Until now, we reported the hausmannite nanorods with secondary plate-like nanostructures [37] and porous hausmannite plates [47] using the galvanostat cathodic deposition, where pulse cathodic deposition method has been applied in this work. The supercapacitive evaluation by CV have indicated that; Mn_3O_4 nanorods with secondary plate like structures were capable to deliver SCs of 298,

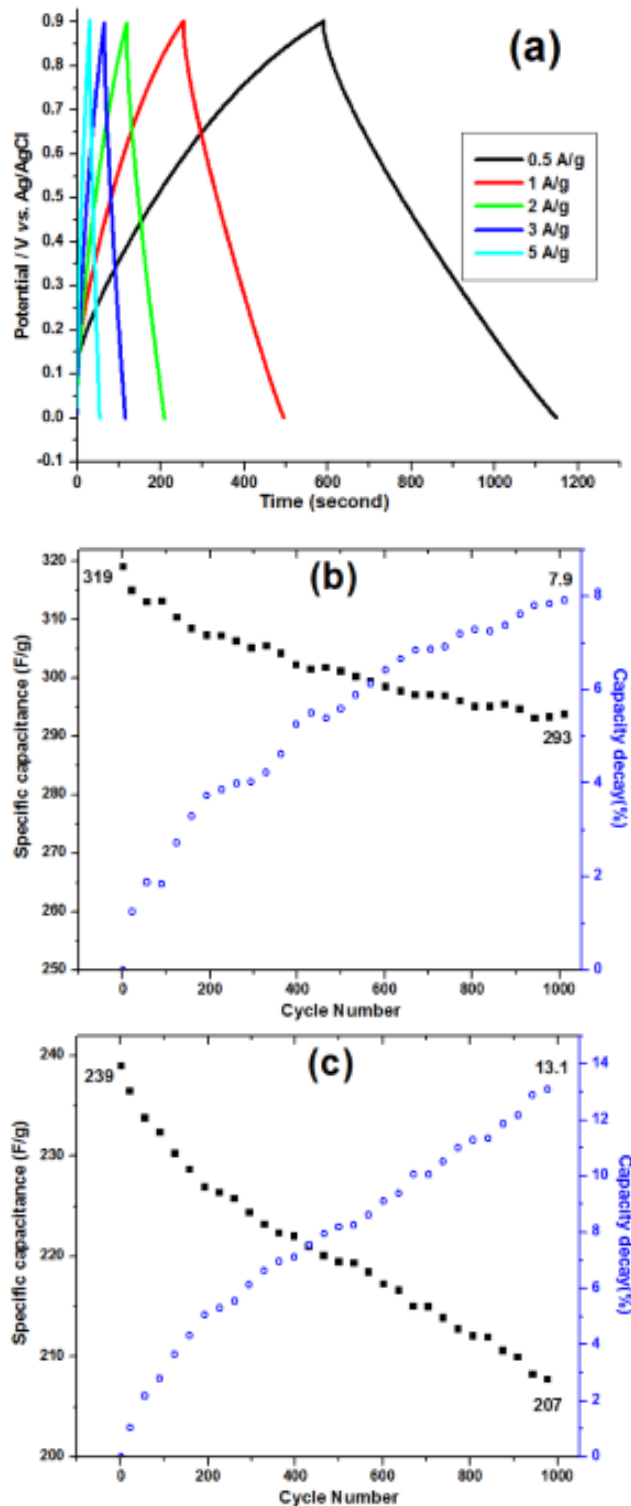


Figure 6. (a) GCD profiles of the fabricated hausmannite working electrode at the different applied current loads, and specific capacitance and capacity decay during 1000 GCD cycles at the current loads of (b) 0.5 and (c) 2 A g^{-1}

258, 218, 189 and 152 F g⁻¹ at the scan rates of 2, 5, 10, 25 and 50 mV s⁻¹, respectively, as reported in Ref. [37], and the porous Mn₃O₄ plates exhibit SCs of 341, 318, 284, 232, 197 and 142 F g⁻¹ at the scan rates of 2, 5, 10, 25, 50 and 100 mV s⁻¹, respectively, as reported in Ref. [47]. Furthermore, the Mn₃O₄ nano-rods/particles, prepared in this work, deliver SCs of 322, 298, 273, 217, 182, 152 and 134 F g⁻¹ at the scan rates of 2, 5, 10, 25, 50 and 100 mV s⁻¹, respectively. Comparing these SC values of these three-type of hausmannite nanomaterials clearly verify the effect of deposition type (i.e. direct or pulse) and morphology on its electrochemical performance of hausmannite.

The galvanostatic charge-discharge (GCD) test is a reliable analysis to evaluate the capacitive performance of any electrode material. Fig. 6a shows GCD profiles of Mn₃O₄ working electrode at the current loads of 0.5, 1, 2, 3 and 5 A g⁻¹. The GCD profiles are symmetric at all the applied current loads indicating the good discharge ability of the prepared electrode materials. Using Eq. (2), the SCs of the fabricated hausmannite working electrode determined to be 311, 276, 239, 190 and 135 F g⁻¹ at the applied currents of 0.5, 1, 2, 3 and 5 A g⁻¹, respectively. These values confirmed the good electrochemical performance of the prepared electrode. Also the capacitance values, calculated from the charge-discharge curves were in agreements with the calculated ones from the CVs (Fig. 5b).

The fabricated Mn₃O₄ electrode was also cycled at the current loads of 0.5 and 2 A g⁻¹, and the SC values and capacity decay during 1000 GCD cycling were calculated, which the results are shown in Figs. 6b and c. The calculations indicated that the SC value of Mn₃O₄ working electrode is reduced from 311 F g⁻¹ to 293 F g⁻¹ after 1000 GCD cycling at 0.5 A g⁻¹, which shows about 7% capacity decay, as seen in Fig. 6b. Also, the Mn₃O₄ working electrode exhibits only 13% capacity decay after 1000 cycles at the current load of 2 A g⁻¹, where its SC value is changed from 239 F g⁻¹ to 207 F g⁻¹ (Fig. 6c). These results confirmed the stable capacitance behaviors of our prepared electrode material during cycling. Hence, the prepared Mn₃O₄ nano-rods/particles can be a suitable electrode material for supercapacitors.

4. CONCLUSION

Hausmannite nano-rods/particles were prepared *through* pulse cathodic deposition in the presence of an anionic surfactant i.e. CTAB. The pure Mn₃O₄ phase and mixed rod/particle morphology of the electro-synthesized material were proved by XRD, SEM and FT-IR analyses. The prepared Mn₃O₄ was used as supercapacitor electrode material, and its charge storage ability was investigated through cyclic voltammetry and charge-discharge techniques. The fabricated electrode was capable to deliver specific capacitances of 322, 298, 273, 217, 182, 152 and 134 F g⁻¹ at the scan rates of 2, 5, 10, 25, 50 and 100 mV s⁻¹, respectively. These results proved that the Mn₃O₄ nano-rods/particles are proper candidate for use in supercapacitor applications.

REFERENCES

- [1] A. González, E. Goikolea, J. Andoni Barrena, R. Mysyk, Renewable Sustainable Energy Rev., 58, 1189 (2016).
- [2] C. Zhong, Y. Deng, W. Hu, J. Qiao, L. Zhang, J. Zhang, Chem. Soc. Rev., 44, 7484 (2015).
- [3] H. Mohammad Shiri, M. Aghazadeh, J. Electrochem. Soc., 159, E132 (2012).
- [4] A. Barani, M. Aghazadeh, M.R. Ganjali, B. Sabour, A.A. Malek Barmi, S. Dalvand, Mater. Sci. Semicond. Process, 23, 85 (2014).
- [5] M. Kundu, G. Karunakaran, D. Kuznetsov, Powder Technol., 311, 132 (2016).
- [6] M. Aghazadeh, J. Mater. Sci.: Mater. Electron., 28, 3108 (2017).
- [7] L. Junqing, S. Jingli, Y. Xi, Z. Xiaoling, T. Zechao, G. Quangui, L. Lang, Int. J. Electrochem. Sci., 7, 2214 (2012).
- [8] M. Aghazadeh, A. Rashidi, M.R. Ganjali, Int. J. Electrochem. Sci., 11, 11002 (2016).
- [9] W. Sun, X. Rui, M. Ulaganathan, S. Madhavi, Q. Yan, J. Power Sources, 295, 323 (2015).
- [10] M. Aghazadeh, A.N. Golikand, M. Ghaemi, Int. J. Hydrogen Energy, 36, 8674 (2011).
- [11] M. Aghazadeh, M. Ghaemi, B. Sabour, S. Dalvand, J. Solid State Electrochem., 18, 1569 (2014).
- [12] M. Aghazadeh, B. Sabour, M.R. Ganjali, S. Dalvand, Appl. Surf. Sci., 313, 581 (2014).
- [13] J. Tizfahm, B. Safibonab, M. Aghazadeh, A. Majdabadi, B. Sabour, S. Dalvand, Colloids Surf. A, 443, 544 (2014).
- [14] P. Razmjoo, B. Sabour, S. Dalvand, M. Aghazadeh, M.R. Ganjali, J. Electrochem. Soc., 161, D293 (2014).
- [15] M. Aghazadeh, M. Hosseinfard, B. Sabour, S. Dalvand, Appl. Surf. Sci., 287, 187 (2013).
- [16] M. Aghazadeh, J. Appl. Electrochem., 42, 89 (2012).
- [17] M. Aghazadeh, A. Rashidi, P. Norouzi, Int. J. Electrochem. Sci., 11, 11016 (2016).
- [18] J. Tizfahm, M. Aghazadeh, M. Ghannadi Maragheh, M.R. Ganjali, P. Norouzi, F. Faridbod, Mater. Lett., 167, 153 (2016).
- [19] H.R. Naderi, P. Norouzi, M.R. Ganjali, Appl. Surf. Sci., 366, 552 (2016).
- [20] M. Aghazadeh, M. Asadi, M. Ghannadi Maragheh, M.R. Ganjali, P. Norouzi, F. Faridbod, Appl. Surf. Sci., 364, 726 (2016).
- [21] Z.J. Li, T.X. Chang, G.Q. Yun, Y. Jia, Powder Technol., 224, 306 (2012).
- [22] M. Aghazadeh, A.A. Malek Barmi, D. Gharailou, M.H. Peyrovi, B. Sabour, F. Najafi, Appl. Surf. Sci., 283, 871 (2013).
- [23] M. Aghazadeh, S. Dalvand, J. Electrochem. Soc., 161, D18 (2012).
- [24] M. Aghazadeh, R. Ahmadi, D. Gharailou, M.R. Ganjali, P. Norouzi, J. Mater. Sci.: Mater. Electron., 27, 8623 (2016).
- [25] J.T. Mehrabad, M. Aghazadeh, M.G. Maragheh, M.R. Ganjali, P. Norouzi, Mater. Lett., 184, 223 (2016).
- [26] M. Aghazadeh, H.M. Shiri, A.A.M. Barmi, Appl. Surf. Sci., 273, 237 (2013).
- [27] A.A.M. Barmi, M. Aghazadeh, B. Arhami, H.M. Shiri, A.A. Fazl, E. Jangju, Chem. Phys. Lett., 541, 65 (2012).
- [28] M. Aghazadeh, A.A.M. Barmi, T. Yousefi, J. Iranian Chem. Soc., 9, 225 (2012).
- [29] C. Wan, M. Cheng, Q. Zhang, N. Jia, Powder Technol., 235, 706 (2013).

- [30]M. Aghazadeh, M. Ghannadi Maragheh, M.R. Ganjali, P. Norouzi, D. Gharailou, F. Faridbod, *J. Mater. Sci.: Mater. Electron.*, 27, 7707 (2016).
- [31]M. Aghazadeh, M. Asadi, M.G. Maragheh, M.R. Ganjali, P. Norouzi, F. Faridbod, *Appl. Surf. Sci.*, 364, 726 (2016).
- [32]J. Tizfahm, M. Aghazadeh, M.G. Maragheh, M.R. Ganjali, P. Norouzi, and F. Faridbod, *Mater. Lett.*, 167, 153 (2016).
- [33]M. Aghazadeh, M. Ghannadi Maragheh, M.R. Ganjali, P. Norouzi, *RSC Adv.*, 6, 10442 (2016).
- [34]M. Aghazadeh, M. Asadi, M. R. Ganjali, P. Norouzi, B. Sabour, M. Emamalizadeh, *Thin Solid Films*, 634, 24 (2017).
- [35]L. Wang, L. Chen, Y. Li, H. Ji, G. Yang, *Powder Technol.*, 235, 76 (2013).
- [36]S. Guo, M. Zhang, G. Zhang, L. Zheng, L. Kang, Z.H. Liu, *Powder Technol.*, 228, 371 (2012).
- [37]M. Aghazadeh, A. Bahrami-Samani, D. Gharailou, M. Ghannadi Maragheh, M.R. Ganjali, P. Norouzi, *J. Mater. Sci.: Mater. Electron.*, 27, 11192 (2016).
- [38]M. Aghazadeh, I. Karimzadeh, M.R. Ganjali, *J. Mater. Sci.: Mater. Electron.*, (2017) doi:10.1007/s10854-017-7192-z.
- [39]L. Wang, X. Zhang, S. Wang, Y. Li, B. Qian, X. Jiang, G. Yang, *Powder Technol.*, 256, 499 (2014).
- [40]K. Zhang, X. Han, Z. Hu, X. Zhang, Z. Tao, J. Chen, *Chem. Soc. Rev.*, 44, 699 (2015).
- [41]M. Huang, F. Li, F. Dong, Y. X. Zhang, L.L. Zhang, *J. Mater. Chem. A*, 3, 21380 (2015).
- [42]J.G. Wang, F. Kang, B. Wei, *Prog. Mater. Sci.*, 51,74 (2015).
- [43]I. Karimzadeh, M. Aghazadeh, M.R. Ganjali, P. Norouzi, T. Doroudi, *Mater. Lett.*, 189, 290 (2017).
- [44]I. Karimzadeh, M. Aghazadeh, M.R. Ganjali, P. Norouzi, S. Shirvani-Arani, *Mater. Lett.*, 179, 5 (2016).
- [45]I. Karimzadeh, M. Aghazadeh, M.R. Ganjali, T. Doroudi, *Curr. Nanosci.*, 13, 167 (2016).
- [46]J. Liu, J. Liu, W. Song, F. Wang, Y. Song, *J. Mater. Chem. A*, 2, 17477 (2014).
- [47]M. Aghazadeh, M. Hosseinifard, B. Sabour, S. Dalvand, *Appl. Surf. Sci.* 287, 187 (2013).